Spallation of Cu by 3.9-GeV ^{14}N ions and 3.9-GeV protons*

J. B. Cumming, P. E. Haustein,† and R. W. Stoenner
Chemistry Department, Brookhaven National Laboratory, Upton, New York 11973

L. Mausner and R. A. Naumann
Chemistry Department, Princeton University, Princeton, New Jersey 08540

(Received 15 April 1974)

Relative yields of 35 products extending from ^{3}H to ^{76}Br have been measured for the interaction of 3.9-GeV (278-MeV/amu) ^{14}N ions with copper. For purposes of comparison, cross sections of 54 nuclides produced by the irradiation of Cu with 3.9-GeV protons are also reported. Although the over-all patterns of yields for ^{14}N ions and protons are qualitatively similar, there are significant differences. In the mass region $37 \leq A \leq 64$, the mass yield curve for ^{14}N ions decreases more rapidly with decreasing A than does the proton curve. No difference could be detected in the shapes of the charge dispersion curves. However, the data indicate a small shift (< 0.1 Z unit) favoring neutron-deficient products near the target in the case of ^{14}N ions. The mass yield curves appear to have similar shapes from $A \approx 40$ down to $A \approx 24$, but formation of the still lighter products, ^{7}Be and particularly ^{3}H, is favored in the ^{14}N irradiation. An observed enhancement of products such as ^{62}Zn, ^{66}Ga, and ^{69}Ge is interpreted as arising largely from secondary reactions rather than from primary processes which add charge or mass from the ^{14}N to the target nuclei. Some discussion of results from this and other experiments with high-energy protons and heavy ions with complex nuclei is presented in terms of the concepts of limiting fragmentation and factorization.

[NUCLEAR REACTIONS Cu(^{14}N, spallation), $E = 3.9$ GeV; measured relative $\sigma(A, Z)$, 35 products ^{3}H–^{76}Br. Cu(p, spallation), $E = 3.9$ GeV; measured $\sigma(A, Z)$, 54 products ^{3}H–^{69}Ge. Natural targets, Ge(Li), β counting, radiochemistry.]

I. INTRODUCTION

The successful acceleration of heavy ions to relativistic energies (100–2000 MeV/amu) at the Princeton particle accelerator[1] and the Berkeley Bevatron[2] has opened a broad new area for study in the laboratory. Except for the lighter ions up to ^{4}He, heavy ion acceleration was previously limited to energies of ≈10 MeV/amu. While a great number of experiments have been reported using such low-energy heavy ions, it was not possible to study spallation and fission with heavy ions in the multi-GeV range for comparison with protons with these energies. Such processes are of great importance to our understanding of the energy and momentum transfer and deexcitation processes which occur when groups of nucleons interact with complex nuclei, and for our understanding of heavy cosmic ray interactions with matter.

Early studies of reactions of multi-GeV heavy ions have indicated that significantly different processes are important at these energies compared to those at 10 MeV/nucleon. For example, fragmentation of projectiles has been observed[3-6] to lead to particles of lower mass and charge which have very nearly the same velocity and direction as the incident ion. The spectra and relative yields of projectile fragmentation products do not appear to depend on the target nucleus.[4]

Fission of heavy elements[7] by high-energy heavy ions is enhanced over that observed for protons by a factor which may be larger than that expected from purely geometrical arguments. A characteristic feature of ^{14}N induced fission is the rapid decrease in momentum transfer associated with the fission process as the ion energy is increased from 4 to 29 GeV, approaching a situation similar to that observed for energetic protons.

It has been observed[8] that light fragments are more copiously produced in heavy ion irradiations of gold, that such fragments have lower mean energies and charges, and that the minimum energies of the fragments are lower than from irradiations with protons having the same kinetic energy/nucleon. This led to the conclusion that more energy is deposited in the nucleus by heavy ions.

Largely because of low beam intensities, previous work has emphasized the use of track detectors or electronic techniques for the detection of light products or fission fragments from the interaction

of very-high-energy heavy ions.[9] The present work, based on the assay by absolute γ and β counting of the radioactivities induced in copper by 3.9-GeV ^{14}N ions, provides what we believe to be the first comprehensive investigation of spallation by heavy ions at GeV energies. We were able to examine a variety of products extending from ^{3}H to ^{76}Br. For purposes of comparison, similar data were also obtained for 3.9-GeV protons.

II. EXPERIMENTAL PROCEDURES AND RESULTS

Three copper targets were irradiated for 290 min in the external 3.9-GeV (278-MeV/amu) ^{14}N ion beam of the Princeton particle accelerator (PPA). Each target consisted of three discs of high purity[10] Cu (1.6 cm in diam, 345 mg/cm^2 thick) which were held together by a wrapping of 10.5-mg/cm^2 Cu. The thickness of these targets was selected as a compromise between activity production and energy loss of the beam. Schimmerling, Vosburgh, and Todd[11] have observed that the measured energy losses of ^{14}N ions in polyethylene, Al, and Pb agree with those calculated from proton data[12] by the application of stopping power theory. We estimate from the data for protons in copper that the energy loss in one of our 1.06 g/cm^2 targets was $\approx$135 MeV. We also estimate that nuclear attenuation was $\approx$3%.

The targets denoted $N1$, $N2$, and $N3$, were spaced in that order at $\approx$30 cm intervals along the beam line to reduce the effects of secondary particles. At the time of the irradiation the beam could not be focused to the size anticipated and it was necessary to center the targets in a beam larger than their diameters. Polaroid film was used for alignment. Our results indicate all three targets were exposed to essentially identical fluxes. The average beam intensity as reported by the PPA staff was $\approx 3\times10^5$ ^{14}N ions/sec. (Only part of this was intercepted by the targets.)

After irradiation, targets $N1$ and $N3$ were flown to Brookhaven (BNL) while $N2$ was retained at Princeton (PU). $N1$ was dissolved and subjected to radiochemical analysis with special emphasis being placed on the recovery of the elements Zn, Ga, Ge, and Br which represent addition of charge from the ^{14}N ions to the target, and on ^{64}Cu, a simple reaction product which could not be detected readily by gross-γ counting. $N1$ was selected for this analysis as the flux of secondary particles resulting from the fragmentation of the ^{14}N ions (which could also form $Z>29$ products) was expected to be lower in $N1$ than in the targets further downstream.

The chemically separated sources were assayed with low-level β counters having efficiencies from $\approx$10 to $\approx$60% depending on β energy and sample thickness, and backgrounds of $\approx$0.3 cpm. Efficiency vs sample thickness curves for these detectors were experimentally obtained for ^{46}Sc, ^{64}Cu, ^{11}C, ^{32}P, and ^{24}Na, and values for the isotopes of interest were obtained by interpolation. Decay curves of the β samples were analyzed by the least-squares program CLSQ.[13] Several elements of lower atomic number than copper were also chemically separated as checks on the γ-ray measurements of targets $N2$ and $N3$.

The three discs of $N3$ were assayed at BNL with a highly efficient $\approx$70 cm^3 Ge(Li) detector (resolution $\approx$1.9 keV at 1332 keV) and a 4096-channel pulse height analyzer. The first count started 99 min from the end of irradiation. Sequential γ-ray spectra were recorded on magnetic tape for analysis by the BRUTAL program.[14] Decay curves of the resolved peaks were analyzed by CLSQ[13] to give counting rates at the end of irradiation. Hand analyses of some spectra were used to check the computer analyses for some of the stronger γ-ray lines, and to resolve a few of the weaker lines which fell below the peak detection threshold of BRUTAL ($\approx$50% statistical uncertainty).

γ spectra from two discs of the $N2$ target were obtained at Princeton starting 40 min from the end of irradiation using a Ge(Li) detector which had a very similar response-vs-energy curve to that of the Brookhaven detector. (The third disc was subjected to radiochemical analysis similar to $N1$, but the factor of 3 lower intensity led to inconclusive results.) The γ spectra were plotted by machine, location of the peaks to be analyzed was made by hand, and a computer program resolved the indicated peaks from background. A simple least-squares program was used to obtain intensities of the γ-ray lines at the end of irradiation.

Peak efficiency (e_P) and total efficiency (e_T) vs γ-ray energy calibration curves were measured for the PU and BNL high-geometry detectors with a variety of standardized γ sources. The curve at BNL was measured using copper absorbers to closely simulate the 1 g/cm^2 counting sample, that at PU was obtained with uncovered sources. In either case, the necessary corrections for self-absorption were made based on the tabulated mass absorption curves.[15] Representative efficiencies of the BNL detector system for the 1-g/cm^2 sample at 511 keV are $e_P=2.4\%$ and $e_T=10.9\%$. A knowledge of the total efficiencies is essential to correct for γ-ray summing when such high-geometry detectors are used. For example, if a γ ray is preceded by positrons, the nominal peak efficiency for the γ ray must be reduced by $(2\times10.9)\%$ in the above example. Summing corrections based on available decay scheme informa-

tion[16] were applied to all of the data obtained in the present work. The enhanced signal to background ratios and more reliable resolution of peaks favor the use of the highest possible efficiencies, even though summing corrections may be as large as 30% in some cases.

For comparison with the ^{14}N ion data two copper targets, each consisting of three 42-mg/cm^2 Cu foils guarded by 10.5-mg/cm^2 Cu and having stacks of three 6-mg/cm^2 Al foils on the up- and downstream sides, were irradiated with 3.9-GeV protons in the Brookhaven alternating gradient synchrotron (AGS). After irradiation, 1- by 2-cm rectangles were punched from the target stacks $\approx$1 mm back from the leading edge. The three foils ($P1$, $P2$, and $P3$) from one target, which, based on monitor assays, had been exposed to $\approx 2\times 10^{13}$ protons, were distributed in the same way as the foils from the ^{14}N irradiation, with $P1$ and $P3$ retained at BNL and $P2$ being flown to Princeton. For assay of these proton irradiated foils, lower efficiency detectors were used both at BNL and PU because of the higher counting rates. Absolute calibration curves (both peak and total) were available for the BNL detector, but only relative curves for the PU detector. However, by comparison of the results from BNL and PU and by later counting of the $P2$ foil in both the high- and low-geometry systems at BNL, it was possible to place the PU data on an absolute basis. An additional 2% error was applied to the PU data as a consequence of this procedure. Foils from the other target ($P1'$, $P2'$, and $P3'$) which had been irradiated with $\approx 6\times 10^{14}$ protons were assayed with the same detector at BNL which had been used for the ^{14}N studies to obtain cross sections for some of the longer-lived products.

After completion of the γ-ray measurements, hydrogen and argon isotopes were extracted from some of the targets by heating in an atmosphere of 20 mm of O_2. These were chemically purified and assayed in appropriate low-background detector systems. ^{3}H was determined in foils $N2$ and $P3$, and ^{37}Ar in foils $N2$, $N3$, and $P3$. ^{3}H, ^{39}Ar, and ^{42}Ar were measured in all three foils ($P1'$, $P2'$, and $P3'$) of the more active target stack. It was observed in studies of ^{3}H extraction from these more active foils, that a single pass extraction of the type which had been used to assay $N2$ and $P3$ gave only $\approx$50% recovery. Our cross sections for forming ^{3}H by proton bombardment of Cu are based on results of multiple pass extractions. However, for ^{14}N ions, the cross section includes the correction for loss in the single pass extraction. A large error (25%) has been assigned to this ^{3}H cross section as a consequence.

The basic data from these experiments consisted of a large set of counting rates for various β or γ rays extrapolated to the ends of the irradiations. A detailed description of the treatment of these data is given in the Appendix. To summarize, each counting rate was corrected for detector efficiency, γ-ray summing if appropriate, radiation abundance, and temporal variation of the beam to obtain relative production rates. For the proton experiments, these were converted to absolute cross sections on the basis of assays of ^{24}Na in the central Al foil of the upstream stack. The ^{27}Al-$(p, 3pn)^{24}$Na cross section was taken to be 9.0 mb at 3.9 GeV[17] and a 1.6% correction was applied for production of ^{24}Na by secondary particles.[18] Standard deviations assigned to the individual measurements of cross sections included, in addition to the nominal statistical errors from the spectral and decay curve resolutions, the following: a 2% uncertainty for chemical yield determinations; a 4% contribution for reproducibility of the β counts; and, 2% for reproducibility for the γ counts. These extra contributions reflect our experience that reproducibility of measurements is rarely as good as the nominal errors would indicate when the statistical errors are less than a few percent.

For many nuclides we had results of multiple determinations for both ^{14}N and proton irradiations based on the different targets, the two laboratories, different γ rays of a given species, or β counts. In these cases weighted mean cross sections were calculated and internal agreement of the replicate measurements was examined. In a few instances, poor agreement could be traced to a single measurement, and if a valid reason could be found, e.g., a poor decay curve, the value was discarded. In all cases where internal agreement was worse than expected from the error estimates on the individual values, the standard errors of the means have been increased to reflect this fact. Specific examples of agreement or disagreement of replicates are given in the Appendix.

Relative cross sections for forming 35 products from Cu by irradiation with 3.9-GeV ^{14}N ions are reported in Table I. The values in column 2 are the mean saturation disintegration rates (min^{-1}) for our irradiation conditions divided by 10^3. 25 of these entries are based on two or more determinations. For only 4 of these (tagged with a P in Table I) was the agreement of replicates poorer than two times that expected from the error estimates. The ten values based on single determinations are tagged S. One of these, that for ^{65}Ga appears to be highly anomalous and is suspect for reasons described in the Appendix.

The higher activity levels in the proton irradiations allowed the determination of more products, 54 in all, for which cross sections in mb are given

TABLE I. Relative yields, cross sections, and yield ratios for products of the interaction of copper with 3.9-GeV ^{14}N ions and protons. Symbol (S) denotes results of a single determination. Symbol (P) denotes agreement between duplicates was poorer than expected, see text.

Isotope	^{14}N relative yield [a]	Proton cross section (mb)	Ratio ^{14}N/protons
^{3}H	660 ± 165 (S)	155 ± 16	4.26 ± 1.14
^{7}Be	18.8 ± 1.8	13.0 ± 0.7	1.45 ± 0.16
^{22}Na	...	2.81 ± 0.05	...
^{24}Na	3.26 ± 0.20 (P)	3.70 ± 0.09	0.88 ± 0.06
^{27}Mg	...	1.59 ± 0.19	...
^{28}Mg	0.36 ± 0.03	0.45 ± 0.01	0.81 ± 0.07
^{29}Al	...	2.2 ± 0.4 (S)	...
$^{34}Cl^{m}$	...	0.59 ± 0.05 (P)	...
^{38}Cl	...	1.70 ± 0.05	...
^{39}Cl	0.59 ± 0.14	0.64 ± 0.02	0.92 ± 0.22
^{37}Ar	3.91 ± 0.09	4.62 ± 0.10	0.85 ± 0.02
^{39}Ar	...	7.00 ± 0.16	...
^{41}Ar	0.61 ± 0.05	0.82 ± 0.02	0.74 ± 0.07
^{42}Ar	...	0.172 ± 0.004	...
^{42}K	2.50 ± 0.10	3.59 ± 0.17 (P)	0.70 ± 0.04
^{43}K	0.97 ± 0.04	1.32 ± 0.04	0.73 ± 0.03
^{44}K	...	0.12 ± 0.04 (S)	...
^{47}Ca	...	0.09 ± 0.02 (S)	...
^{43}Sc	3.35 ± 0.16	4.11 ± 0.08	0.82 ± 0.04
$^{44}Sc^{m}$	4.22 ± 0.06	5.22 ± 0.11	0.81 ± 0.02
$^{44}Sc^{g}$	2.94 ± 0.18	4.41 ± 0.24 (P)	0.67 ± 0.05
^{46}Sc	5.46 ± 0.23	6.34 ± 0.18	0.86 ± 0.04
^{47}Sc	1.82 ± 0.05	2.39 ± 0.14	0.76 ± 0.05
^{48}Sc	0.44 ± 0.05	0.65 ± 0.02	0.68 ± 0.08
^{48}V	8.6 ± 0.5	9.0 ± 0.1	0.96 ± 0.06
^{48}Cr	0.30 ± 0.02	0.31 ± 0.01	0.98 ± 0.06
^{49}Cr	2.42 ± 0.23	2.47 ± 0.04	0.98 ± 0.09
^{51}Cr	18.8 ± 1.0	19.3 ± 0.6	0.98 ± 0.06
$^{52}Mn^{m}$	...	0.18 ± 0.01 (S)	...
$^{52}Mn^{g}$	5.49 ± 0.21 (P)	6.08 ± 0.07	0.90 ± 0.04
^{54}Mn	13.2 ± 1.3	13.8 ± 0.2	0.96 ± 0.09
^{56}Mn	2.21 ± 0.06	2.58 ± 0.08 (P)	0.86 ± 0.05
^{52}Fe	...	0.18 ± 0.02 (S)	...
^{53}Fe	...	1.83 ± 0.22 (S)	...
^{59}Fe	...	1.33 ± 0.24	...
^{55}Co	1.04 ± 0.08	0.97 ± 0.07 (P)	1.06 ± 0.12
^{56}Co	7.0 ± 0.4	5.6 ± 0.3 (P)	1.25 ± 0.10
^{57}Co	15.7 ± 1.1	16.9 ± 0.1	0.93 ± 0.06
^{58}Co	22.4 ± 0.8	20.6 ± 0.2	1.09 ± 0.04
^{60}Co	...	8.34 ± 0.09	...
^{61}Co	3.10 ± 0.14 (S)	4.00 ± 0.08	0.78 ± 0.04
^{62}Co	...	0.51 ± 0.04	...
^{56}Ni	...	0.14 ± 0.08 (S)	...
^{57}Ni	0.59 ± 0.06 (S)	0.66 ± 0.06 (P)	0.90 ± 0.12
^{65}Ni	...	0.46 ± 0.07 (S)	...
^{60}Cu	...	1.92 ± 0.06	...
^{61}Cu	13.7 ± 0.8 (P)	11.5 ± 0.4 (P)	1.19 ± 0.08
^{64}Cu	15.0 ± 1.6 (S)	14.3 ± 0.7 (S)	1.04 ± 0.12
^{62}Zn	0.65 ± 0.02	0.126 ± 0.005	5.33 ± 0.24
^{63}Zn	...	1.9 ± 0.4 (S)	...
^{65}Zn	...	0.67 ± 0.06	...
^{65}Ga	[4.8 ± 0.7 (S)] [b]	0.11 ± 0.09 (S)	...
^{66}Ga	0.28 ± 0.02 (S)	0.099 ± 0.005 (S)	2.83 ± 0.27
^{69}Ge	0.059 ± 0.006 (S)	0.010 ± 0.002 (S)	5.6 ± 1.1
^{76}Br	0.006 ± 0.003 (S)	...	...

[a] Values are saturation disintegration rates (min^{-1}) divided by 10^{3}.

[b] This value is suspect, see Appendix.

in Table I. 9 of these are class P results and 15 class S. For several of the longer-lived products, the tabulated value is the mean of determinations in the foils of two independent irradiations, e.g., the value for ^{54}Mn is based on the assay of foils $P2$ and $P3$ from one irradiation at BNL and PU, and foils $P1'$, $P2'$, and $P3'$ from the other at BNL. Agreement of cross sections from the duplicate irradiations was 2.4% or better for ^{22}Na, ^{54}Mn, ^{57}Co, ^{58}Co, and ^{60}Co, 6% for ^{46}Sc, and 15% for ^{56}Co. Source of the last discrepancy could not be determined, but it is reflected in the large error assigned the ^{56}Co cross section in Table I. All cross sections in Table I are effectively cumulative except in those cases where a long-lived or stable precursor blocks β decay. However, examination of the data indicates β decay feeding is in general a small effect.

The proton cross sections obtained in this work confirm the general pattern[19,20] of yields of the spallation of light elements by GeV protons. Isotopic yield distributions are plotted for Co in Fig. 1 and for Sc in Fig. 2. For a given element the largest cross sections are found slightly to the neutron-deficient side of β stability. Cross sections appear to decrease by about a factor of 2 in going from Co to Sc. The shape of the isotopic distribution for Co appears skewed on the heavy mass side, possibly a consequence of the proximity of these products to the target nuclei ^{63}Cu and ^{65}Cu.

Relative yields from the ^{14}N-ion irradiations are also plotted in Figs. 1 and 2. As a consequence of the arbitrary normalization of the ^{14}N data in Table I, results for ^{55}Co to ^{58}Co fall very nearly on the same curve as for protons. However, the yield of ^{61}Co in the ^{14}N ion irradiation is $\approx$25% lower. All five Sc yields fall $\approx$25% below the corresponding proton values.

Yield ratios (relative yields for ^{14}N ions/proton cross sections) from Table I are plotted as a function of product mass in Fig. 3. The solid curve in this figure indicates a generally increasing yield ratio with increasing mass above $A=37$ for neutron-deficient products (filled circles). On the other hand, ratios for the neutron-rich products (open circles in Fig. 3) from ^{24}Na to ^{61}Co are essentially constant. This suggests a shift of the

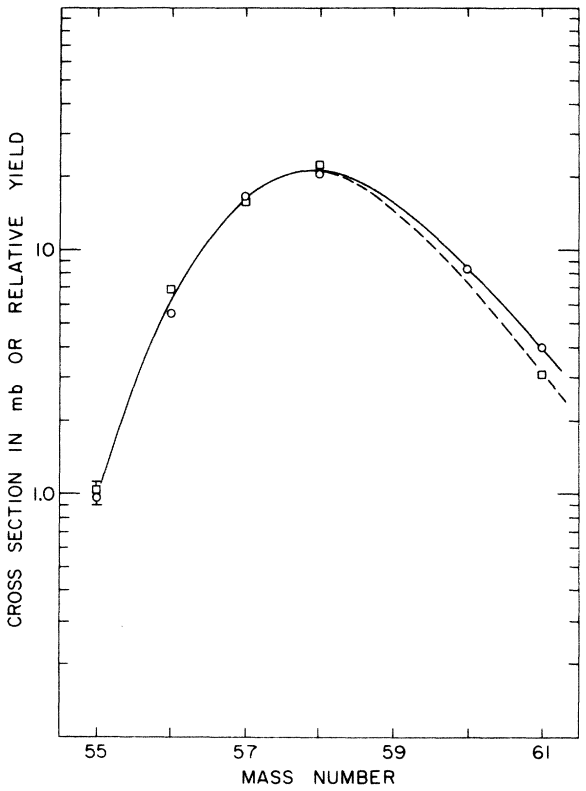

FIG. 1. Relative yields of Co isotopes observed in the interaction of 3.9-GeV ^{14}N ions and protons with Cu. The solid curve and circles give cross sections in mb for protons. The dashed curve and squares give relative yields for ^{14}N ions.

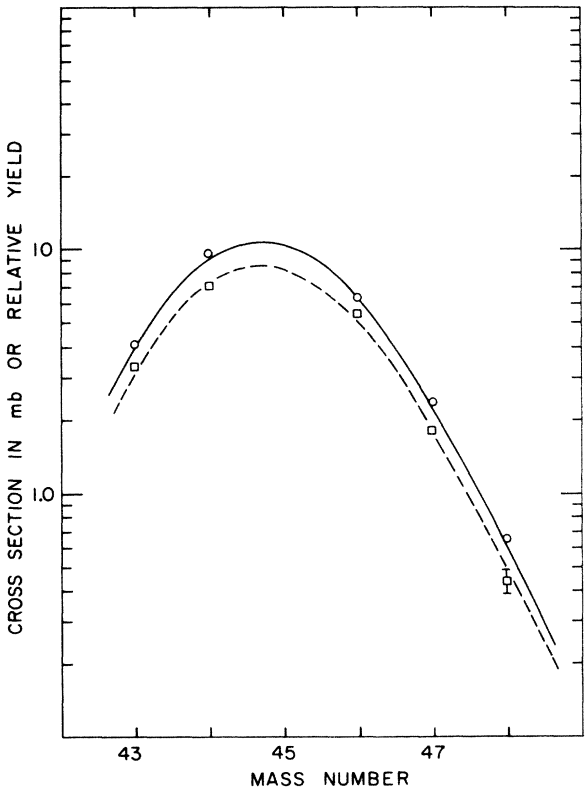

FIG. 2. Relative yields of Sc isotopes observed in the interaction of 3.9-GeV ^{14}N ions and protons with Cu. The solid curve and circles give cross sections in mb for protons. The dashed curve and squares give relative yields for ^{14}N ions.

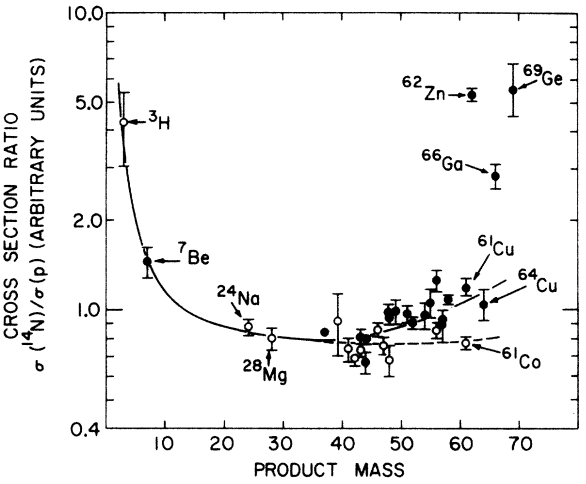

FIG. 3. Dependence of observed cross section ratios on product mass for the 3.9-GeV ^{14}N ion and proton spallation of copper. Neutron-deficient isotopes are indicated with filled circles, neutron-rich are open. The solid curve indicates the general trend of these data. The dashed curve suggests less variation for the neutron-rich products.

charge dispersion curve of 3.9-GeV ^{14}N ions relative to that for 3.9-GeV protons so as to slightly favor neutron-deficient products within ≈20 mass numbers of the target. This is just opposite to the conclusion drawn by Karol[21] from a comparison of yields of the spallation of Cu by 720-MeV α particles with those of comparable energy protons.[22] A more detailed analysis and discussion of the results from the present experiment will be presented below.

III. ANALYSIS AND DISCUSSION

A. Mass and charge distributions

In an experiment such as the present one, many yields, e.g., those of stable or long-lived products, are not measured. To proceed further with the analysis of our results, a method for estimating the missing yields must be developed. We will proceed in the general direction formulated by Rudstam,[23] namely to seek simple analytical functional forms which approximate the spallation yield distribution. We assume,

$$\ln[\sigma(A, Z)] = Y(A) + C(Z_p(A) - Z), \quad (1)$$

where $\sigma(A, Z)$ is the cross section in mb (or relative yield) of a product of mass and atomic number A and Z. The function $Y(A)$ determines the distribution of total isobaric yields. (What is commonly called the mass yield curve is given by $e^{Y(A)}$.) The function $C(Z_p(A) - Z)$ describes the distribution of yields at a given mass number with $e^{C(Z_p(A)-Z)}$ representing the charge dispersion curve. In this parametrization it is assumed that the shape of the normalized charge dispersion curve does not depend on A when measured relative to a reference atomic number $Z_p(A)$ at each A. For spallation, it is convenient to consider $Z_p(A)$ to be the position of the maximum yield at the mass number A. The availability of a nonlinear least-squares program on a high speed digital computer allowed the testing of a variety of forms for the functions Y, C, and Z_p and the adjustment of the free parameters for optimum fit to the experimental data. We started with the proton cross sections (Table I) since more data, particularly on the wings of the distribution, were available for protons than for ^{14}N ions, and we limited the range of masses initially to $37 \leq A \leq 57$. Only a few yields were measured for lower masses, and specific effects of the two target nuclei, ^{63}Cu and ^{65}Cu, were expected at higher masses. The procedure was to fit a given model, to examine the statistical significance of its terms and the quality of fit, and then to drop insignificant terms and/or modify the function to achieve an improved fit to the data. By this procedure we first arrived at a six parameter model which was then broadened to include the data up to mass 61. Similar but less detailed analyses of the ^{14}N ion data were performed. From comparisons of the ^{14}N data with results for the same isotopes by protons it was shown that the shape of the charge distributions for the two bombarding particles were indistinguishable but that the Y and Z_p functions were different. It was also shown that the shape of the charge distribution determined from all the proton data could be forced upon the ^{14}N data with no detriment to the quality of fit. We present the final conclusions from these analyses below.

1. *Function Z_p*

It is clear that the function $Z_p(A)$ plays a very important role in Eq. (1) as it locates the position of the maximum yield at each A. As it had been noted[24] that parametrization of some charge dispersion curves gave satisfactory results in terms of $Z_A - Z$, where Z_A is the position of the line of β stability at mass A, we started with the assumption that $Z_p(A)$ was shifted by an adjustable constant amount from $Z_A(A)$. Values of $Z_A(A)$ were calculated from the mass tables of Garvey *et al.*[25] It rapidly became apparent that this approach was not satisfactory for copper spallation yields. The reason for this can be seen in Fig. 4. The heavy dashed curve traces Z_A on the Z, N plane. Location of the target nuclei ^{63}Cu and ^{65}Cu are also shown. The Z_A curve shows oscillations as a consequence of the shells at N and Z equal to 20

and to 28. The points in Fig. 4 are our estimates of the positions of maximum yields based on plots of isotopic, isotonic, or isobaric series, e.g., Figs. 1 and 2, for the proton cross sections. It is clear that the ridge line of the spallation distribution is much less affected by shell structure than is the Z_A curve; accordingly we did not pursue the Z_A approach. Rather, a simple polynomial expansion[26] in $(A-50)$ was assumed for Z_P. It was shown that inclusion of terms beyond linear did not significantly improve the quality of the fit to the experimental data either for protons or ^{14}N ions, and we use the form

$$Z_P(A) = X_1 + X_2(A-50). \quad (2)$$

Values of X_1 and X_2 for protons and for ^{14}N from the present work are given in Table II. For comparison, values deduced by Barr[27] and Rudstam[23] are also included. As they assumed different functional forms for Z_P, we have calculated from their equations values appropriate for $A=50$. The differences seen in the table, although small will have significant effects on the wings of the charge dispersion curves.

Another way to obtain Z_P values (which is independent of mass yield curves) is to compare experimental isobaric yield ratios with those calculated from a charge dispersion curve. This procedure is illustrated in Fig. 5 for the ratio ^{61}Cu/^{61}Co. The solid curve is that calculated from our "best" charge dispersion curve (see below). The boxes are regions consistent with the experimentally measured ratios. It can be concluded that $Z_P(61)$ is 28.20 ± 0.01 for protons and 28.28 ± 0.02 for ^{14}N ions. Extrapolation of the linear form, Eq. (2), would have given values of 28.44 and 28.45, respectively. It is clear that deviations from the linear form such as shown by the solid curve in Fig. 4 are necessary near the target and these were incorporated in our final analysis.

Results from similar analyses of ratios at $A=56$, 48, and 43 are presented in Table III. The Z_P differences $[Z_P(^{14}\text{N}) - Z_P(^{1}\text{H})$ as given in column 5] are small, <0.1 Z unit, and appear to decrease with increasing distance from the target. Of course, a pronounced shift of the product distribution would be expected for an irradiation with 10-MeV/amu ^{14}N ions as a consequence of $(^{14}\text{N}, xn)$ reactions or transfer reactions. Whether the small shift observed for 3.9-GeV ^{14}N ions represents a residual of such an effect, for example, the transfer of an α particle or two protons followed by neutron evaporation, cannot be uniquely

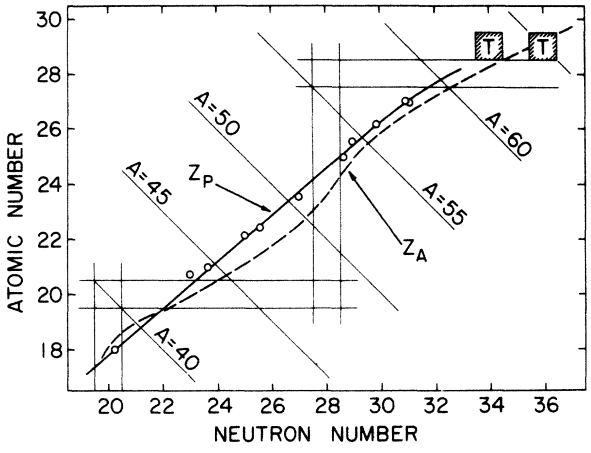

FIG. 4. Locus on the N, Z plane of the ridge line (maximum yields) of the spallation distribution observed in the reaction of Cu with 3.9-GeV protons. The points are estimates of the position of maximum yields based on the experimental data. The heavy solid curve marked Z_P indicates the values derived from the six parameter model discussed in the text. The heavy dashed curve marked Z_A traces the position of β stability in this mass range as derived from the data of Garvey *et al.* (Ref. 25). Positions of the target nuclei ^{63,65}Cu are indicated by T.

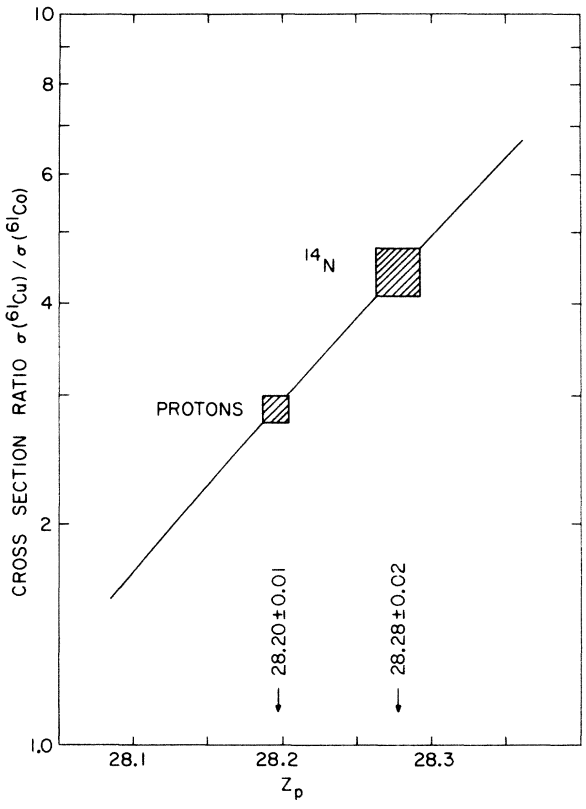

FIG. 5. Determination of Z_P values from experimental isobaric yield ratios for ^{61}Cu/^{61}Co. The curve was calculated from the charge distribution described in the text. The shaded boxes represent regions consistent with the experimental data for ^{14}N ions and for protons as indicated. Derived Z_P values are indicated by arrows pointing to the abscissa.

TABLE II. Parameters of the Z_p function.

Particle, source	X_1	X_2
3.9-GeV protons, this work	23.419 ± 0.014	0.4566 ± 0.0019
3.9-GeV ^{14}N, this work	23.431 ± 0.011	0.4560 ± 0.0018
5.7-GeV protons, Barr [a]	23.35	0.467
3.9-GeV protons, Rudstam [b]	23.34	0.447

[a] Reference 27.

[b] Calculated from the equations given in Ref. 23 for a Gaussian charge dispersion at $A = 50$.

decided. It is interesting, however, that Katcoff and Hudis,[7] in studies of high-energy ^{14}N ion induced fission of heavy elements, have postulated an increase in the mean value of Z^2/A of the excited systems formed by ^{14}N ions compared to those formed by protons. This is in the same direction as observed in the present work.

Karol[21] has studied the spallation of copper by 720-MeV α particles. From a comparison of his cross sections with those obtained for 590-MeV protons,[22] he concluded that yields of highly neutron-deficient products were relatively suppressed in the α particle irradiations (by a factor of ≈ 2). We have used Karol's measured yield ratios at $A = 56$, 48, and 43 to calculate the Z_p values which are given in column 4 of Table III. These values are essentially identical with the values for 3.9-GeV protons, and show no evidence for a shift in the direction opposite to that which we have observed for ^{14}N ions.

2. *Mass yield curves*

The function $Y(A)$ of Eq. (1) defines the mass yield curve for the spallation of copper. Once $Z_p(A)$ is established, $Y(A)$ is not very sensitive to the choice of the function $C(Z_p(A) - Z)$. We have assumed a polynomial in $(A - 50)$ for $Y(A)$ and tested the significance of the terms. As was the case for $Z_p(A)$, no significant improvement in the fit to the data for $A = 37$ to 57 was obtained by adding terms above linear, either for the proton or the ^{14}N data. We adopt the form

$$Y(A) = X_3 + X_4(A - 50), \tag{3}$$

for which the best values of X_3 and X_4 are given in Table IV. The absolute value of X_3 for ^{14}N ions is of course not relevant as we have measured only relative cross sections. However, we see in Table IV that the slope of the mass yield curve (X_4) for ^{14}N ions is significantly greater than that observed for protons of the same energy. Equivalent values of X_3 and X_4 from Barr[27] and Rudstam[23] are also included in Table IV. Barr's value for X_3 was adjusted to reflect a revised monitor cross section (8.7 mb for ^{27}Al(p, $3pn$)^{24}Na compared to the 10.5 mb he had used). Rudstam's value was not so adjusted as it was based on a variety of different measurements. Our value of X_4 for protons probably agrees within errors with the values from Barr and Rudstam. It should also be noted that both these authors used a wider range of data than was used for the present fitting procedure.

Another approach to determining the mass yield curves is to use the computer program only to supply the missing yields which may be added to the observed cross sections at various mass numbers. This is illustrated in Fig. 6 for both proton and ^{14}N spallation of copper. Points are filled when measured cross sections accounted for greater than 50% of the total, and open when they accounted for 25 to 50%. No results are shown where less than 25% of a chain was measured. In all cases, an error equal to 20% of the missing yield was added by quadrature to the error on the observed yield. Agreement between the points and lines based on Eq. (3), is well within these error estimates except at $A = 51$ where the measured cross section of ^{51}Cr seems abnormally high. This is also observed in our ^{14}N ion data and in other spallation studies as well. One possible interpretation is that the abundance of the 320-keV γ ray in the ^{51}Cr decay (we have used 9.8%) should be higher ($\approx 11.6\%$).

The proton mass yield curve in Fig. 6 which

TABLE III. Values of Z_p inferred from isobaric cross section ratios for products of the spallation of Cu by 3.9-GeV ^{14}N ions, 3.9-GeV protons, and 720-MeV α particles.

Cross section ratio	Z_p(^{14}N)	Z_p(^{1}H)	Z_p(^{4}He) [a]	Z_p(^{14}N) − Z_p(^{1}H)
^{61}Cu/^{61}Co	28.28 ± 0.02	28.20 ± 0.01		0.08 ± 0.02
^{56}Co/^{56}Mn	26.21 ± 0.01	26.14 ± 0.01	26.14 ± 0.02	0.07 ± 0.02
^{48}Cr/^{48}Sc	22.55 ± 0.02	22.50 ± 0.01	22.49 ± 0.01	0.05 ± 0.02
^{43}Sc/^{43}K	20.23 ± 0.01	20.21 ± 0.01	20.25 ± 0.03	0.02 ± 0.01

[a] Calculated from data of Ref. 21 for 720-MeV α particles.

TABLE IV. Parameters for the mass yield curves of copper.

Particle, source	X_3	X_4
3.9-GeV protons, this work	2.965 ± 0.028	0.0482 ± 0.0030
3.9-GeV ^{14}N, this work	2.856 ± 0.026	0.0611 ± 0.0036
5.7-GeV protons, Barr [a]	2.848	0.0528
3.9-GeV protons, Rudstam [b]	3.076	0.054 ± 0.002

[a] Reference 27.
[b] Reference 23.

varies smoothly from ≈30 mb/amu at $A = 60$ to ≈10 mb/amu at $A = 37$ is in good agreement with that deduced by Husain and Katcoff[28] from a reanalysis of existing data[18,29] on copper spallation by 3-GeV protons. It does not show evidence for a peak of ≈33 mb at $A \approx 48$ that was deduced from an earlier analysis.[30] Our results also agree with Barr's[27] from $A = 37$ to $A = 57$ as shown by the dashed curve in Fig. 6. We have noted above that the ratio ^{61}Cu/^{61}Co could be fitted by adjusting the Z_P value at $A = 61$. However, neither for protons nor for ^{14}N ions could the magnitudes of these cross sections be fitted if an extrapolation of Eq. (3) was assumed. In both cases we saw evidence of an upturn as has been shown in Fig. 6. Our value for protons and Barr's at $A = 61$ are in good agreement, but his estimates of total yields at $A = 58$, 59, and 60 are significantly higher than the present ones.

Figure 6 confirms what had been noted from Table IV, namely that the slope (X_4) of the ^{14}N mass yield curve is greater than that of the proton curve. Although comparison of our proton data with Barr's does not indicate a significant energy dependence for the slope between 3.9 and 5.7 GeV, Rudstam[23] and Schwarz and Oeschger[31] have concluded from a wider range of data that X_4 varies with bombarding energy approximately as $E^{-0.68}$. On this basis, we conclude that the mass yield curve for 3.9-GeV ^{14}N ions on Cu (for $A \geq 37$) has a shape which would be matched by protons of slightly *lower* energy, i.e., ≈2.8 GeV.

3. *Charge dispersion curves*

Charge dispersion curves for the spallation of Cu by 3.9-GeV protons and ^{14}N ions are presented in Fig. 7. Each measured yield in the mass range $37 \leq A \leq 61$ was corrected for β decay feeding, as appropriate, based on experimental or calculated precursor yields (≲10% corrections) and plotted at its $Z_P - Z$ value as a fraction of the total yield at that mass number (from the solid curves in Fig. 6).

During our numerical analysis of these data we had started with a polynomial form for the function $C(Z_P - Z)$ in Eq. (1). Inclusion of terms above order two (a Gaussian) gave significantly improved fits to the experimental data and indicated the charge dispersion curve was skewed to the neutron-rich side. The Gaussian form seemed quite satisfactory for neutron-deficient products and those near stability. We have retained a quadratic form (Gaussian) for $Z_P - Z \leq X_6$,

$$C(Z_P - Z) = X_5(Z_P - Z)^2 + N_C, \tag{4}$$

and forced a smooth junction to a linear tail for $Z_P - Z > X_6$,

$$C(Z_P - Z) = X_5 X_6[2(Z_P - Z) - X_6] + N_C. \tag{5}$$

Both X_5 and X_6 were optimized by least-squares

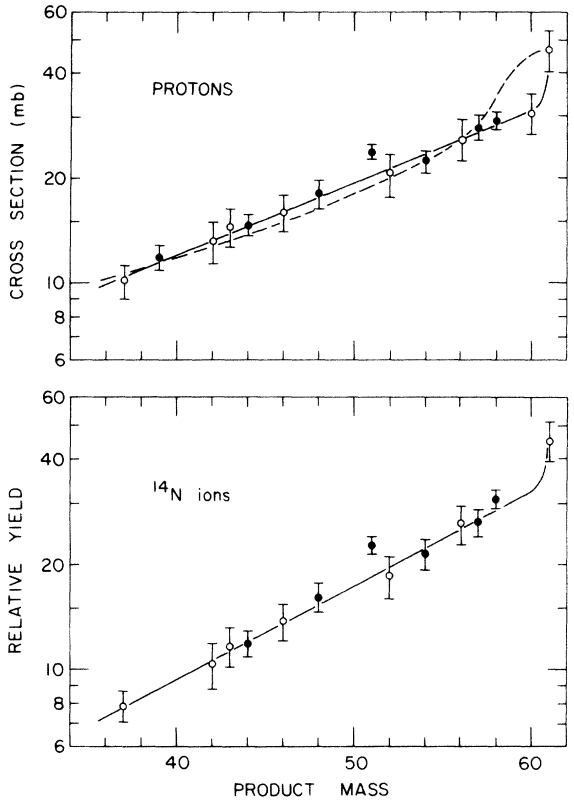

FIG. 6. Mass yield curves for the spallation of copper by 3.9-GeV ^{14}N ions (lower) and protons (upper). The points are the sums of experimentally determined yields with estimates of missing yields from the computer fitting procedure as described in the text. They are filled when the observed yields contributed > 50% to the total and open for 25–50%. The solid curves are computer fits to all the data in this mass region. The dashed curve shown with the proton data is that given by Barr, Ref. 27.

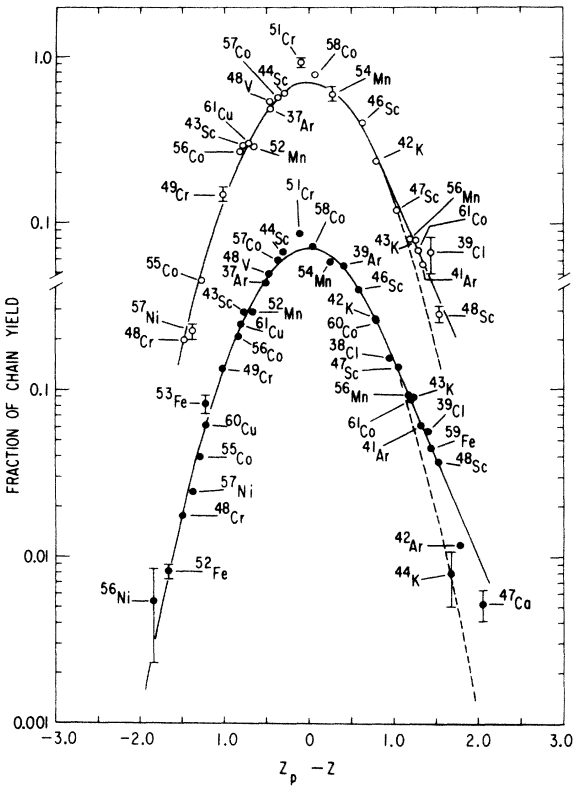

FIG. 7. Charge dispersion curves for products in the mass range $37 \leq A \leq 61$ from the spallation of copper by 3.9-GeV ^{14}N ions and protons. The lower curves and filled points are for protons; the upper curves and open points are for ^{14}N ions. They are displaced vertically by a factor of 10 for display purposes. The curves have identical shapes. The solid curve is that used for the fitting procedure described in the text. The dashed curve is the extension of the Gaussian form used for the central and left parts of the solid curve.

adjustment to the data for protons. N_C is a normalization constant which gives unit area under the charge dispersion curve. Once X_5 and X_6 are obtained by the fitting procedure, N_C is determined by integration. The fitting procedure can only give the sum $(X_3 + N_C)$.

The solid curves in Fig. 7 are defined by Eqs. (4) and (5) with $X_5 = -1.63 \pm 0.05$, $X_6 = 0.83 \pm 0.06$, and $N_C = -0.3461$. The dashed curves are the continuation of the Gaussians. It can be seen that the data points for $1.0 \leq (Z_P - Z) \leq 1.6$ are much better fitted by the tail. However, the most neutron-rich points fall below the tail. While the function defined by Eqs. (4) and (5) is perhaps an oversimplification, it is a good approximation for most of the products. If we omit the one point (^{44}K) which deviates from the curve for protons by more than a factor of 2, the root-mean-square deviation of the other 32 points is ≈19%. The rms deviation for the 21 points for ^{14}N ions is ≈16%. Figure 7 confirms that the charge dispersion curves for protons and ^{14}N ions are identical within errors.

The value of X_5 deduced from the present work is larger than that reported by Barr[27] (1.47) suggesting our charge dispersion curve is narrower. This is largely a consequence of our inclusion of the tail. When a pure Gaussian was forced through the proton data, the value of X_5 was 1.43. If the proton data were analyzed in terms of two half Gaussians, values of $X_5 = 1.68 \pm 0.08$ for the neutron-deficient side and $X_5 = 1.31 \pm 0.06$ for the neutron-rich side were obtained.

From an analysis of a wide range of spallation data, Rudstam[23] concluded that the width parameter should vary as $A^{-0.64}$ for a Gaussian distribution. His formulas give values of $X_5 = 1.31$ at $A = 57$ and $X_5 = 1.72$ at $A = 37$. While some such variations would be expected as a consequence of the broadening of the mass parabolas with increasing A, we see no evidence of this in the mass range examined in the present work.

B. Low and high mass products

Insufficient data are available from the present experiment, particularly in the case of ^{14}N ions, for a detailed analysis of charge dispersion and mass yield curves for products with $A < 37$. From the proton data, we estimate the total isobaric yield at $A = 24$ to be 6.3 ± 0.5 mb. A comparative estimate by Husain and Katcoff[28] is 5.5 mb (at 3 GeV), and by Barr,[27] 6.4 mb (at 5.7 GeV). Extrapolation of Eq. (3) also gives 5.5 mb at $A = 24$, so that to a first approximation Eq. (3) is valid for protons down to that mass. From the nearly identical yield ratios for ^{24}Na and ^{28}Mg (Table I and Fig. 3) and the products at $A \approx 40$, we conclude that the mass yield curves for protons and ^{14}N ions have very similar shapes from $A \approx 24$ to $A \approx 40$. Extrapolation using the steeper slope deduced for ^{14}N ions (Table IV) does not seem appropriate.

For still lighter products, the mass yield curves turn up steeply. Formation of ^{3}H and ^{7}Be, appears to be favored in ^{14}N irradiations compared to protons. For products of mass below that of the projectile, two distinct formation mechanisms are possible. *Projectile fragmentation* is known[3-6] to give products strongly forward peaked with velocities close to that of the incident ^{14}N ion. The ^{7}Be and ^{3}H formed by this mechanism from 278-MeV/amu ^{14}N ions will have ranges [11,12] in Cu of 29 and 200 g/cm^2, respectively. Our 1-g/cm^2 targets are not expected to retain a significant fraction of these products. The other mechanism, *target fragmentation*, is expected to lead to products of lower energy with less forward peaked angular

TABLE V. Variation of some observed cross sections (in mb) with position of foil in the copper targets irradiated with 3.9-GeV protons.

Target position [a]	$\sigma(^3H)$	$\sigma(^7Be)$	$\sigma(^{22}Na)$	$\sigma(^{65}Zn)$
$P1'$	83± 8	···	2.80±0.10	0.61±0.12
$P2'$	100±10	13.2±0.8 [b]	2.76±0.08	0.75±0.10
$P3'$	78± 8	12.2±1.5 [c]	2.89±0.11	0.58±0.12

[a] See text for description of target stacks.
[b] Determined in target $P2$ at PU.
[c] Determined in target $P3$ at BNL.

distributions, in general having similar spectra to those produced by proton irradiation. Only a small recoil loss of target fragmentation products (even ^{3}H) is expected from the 1-g/cm^2 targets of the ^{14}N irradiations.

Unfortunately, the thickness of the targets used in the present proton studies is comparable to the expected range of ^{3}H. Some information on potential recoil losses can be gained from an examination of dependence of measured cross sections on position in the target stack as is shown in Table V. Previous measurements[32,33] indicate our 10.5-mg/cm^2 guard foils will compensate for recoil losses for products at least as light as $A=24$. Results in Table V for ^{22}Na confirm this. With the exception of the results for ^{7}Be, the data in Table V were obtained at BNL under nearly identical circumstances. One ^{7}Be cross section, $P2$, was measured at PU, the other, $P3$, at BNL. A 10.5-mg/cm^2 foil is calculated to compensate for losses of ^{7}Be up to 18 MeV, while the $P2$ foil is guarded by 52.5 mg/cm^2 corresponding to 49 MeV.[34] We believe that the insignificant difference for ^{7}Be seen in Table V is probably due to differences in technique rather than recoil losses.

For ^{3}H, a higher cross section is observed in $P2'$ than in either $P1'$ or $P3'$. Such a difference is expected if the ^{3}H spectrum has appreciable components with ranges from 10.5 to 138 mg/cm^2 of Cu (2.0 to 12 MeV). Several workers[27,35,36] have assumed a mean ^{3}H energy of 12 MeV (range 144 mg/cm^2 in Cu) for making corrections for recoil losses based on some experimental data.[35] A calculated spectrum based on an evaporation model as quoted by Goebel, Schultes, and Zähringer[36] extends from ≈4 to ≈35 MeV with a mean of 12.3 MeV. We have used this spectrum to calculate the apparent retention of evaporated ^{3}H by the foils of our stack and obtain values of 0.54 for $P1$ or $P3$ and 0.60 for $P2$. Application of these corrections to the measured values (Table V) yields a mean cross section of 155± 16 mb. The error reflects our estimate of systematic effects. The relative

TABLE VI. Cross sections for producing ^{3}H by irradiation of copper with high-energy protons.

Proton energy (GeV)	Corrected [a] cross section (mb)	Reference
0.6	52± 3	Goebel *et al.*, Ref. 36
0.66	73±22	Kuznetsov and Mekhedov, Ref. 37
2.2	131± 8	Goebel *et al.*, Ref. 36
3.9	155±16	This work
5.7	167±33	Barr, Ref. 27
25	124±17	Goebel *et al.*, Ref. 36

[a] Cross sections have been corrected where appropriate (or possible) to revised values for the ^{27}Al$(p,3pn)^{24}$Na reaction, see Ref. 17.

yield of ^{3}H reported for ^{14}N ions in Table I also includes a correction (7%) for recoil loss which was calculated in a similar manner. ^{3}H production appears to be strongly enhanced in the ^{14}N irradiation compared to protons. This is consistent with the observation by Sullivan *et al.*[8] of increased light fragment production in the interactions of 34-GeV ^{16}O ions with Au.

Our cross section is compared with other values for ^{3}H production from Cu by GeV protons in Table VI. The apparently small energy dependence between 2.2 and 25 GeV is surprising in view of significant increases in ^{7}Be, ^{22}Na, and ^{24}Na production in the same energy region.[18] It may be of some interest in cosmochemistry that the cross sections for producing ^{3}H from Cu by GeV protons are, on the average, substantially higher than the cross sections from Fe or Ni cited in the review by Kirsten and Schaeffer.[38] Their nine tabulated values for Fe and Ni average only 82 mb. On the basis of an $A^{2/3}$ dependence, only a 10% difference would be expected.

Turning now to the other end of the product mass spectrum, it is well known[39] that the simple reactions (p,pn) and $(p,2p)$ have high yields in proton induced spallation. When the value for ^{64}Cu in Table I is corrected for the isotopic abundance of ^{65}Cu (30.9%) the ^{65}Cu$(p,pn)^{64}$Cu cross section is found to be 46.3± 2.3 mb. We had expected that ^{64}Cu could be formed in ^{14}N irradiations not only by the analogous ejection of a neutron from ^{65}Cu [by a $(^{14}N,^{14}Nn)$ reaction or its equivalent], but also possibly by the transfer of a neutron from the projectile to ^{63}Cu. From the data in Table I and Fig. 3 we see no evidence for any special enhancement (or depletion) of ^{64}Cu yields in the ^{14}N irradiation. The yield ratio for ^{64}Cu (Fig. 3) is similar to those of many other nuclides in the cobalt-copper region. This suggests either that the transfer of a neutron from a 278-MeV/amu ^{14}N is not a significant process, or that, if such transfers

occur, the resultant nuclei must be sufficiently excited to undergo particle evaporation.

We have studied some products with $Z > 29$ to look for effects of more complex transfer reactions in ^{14}N-ion bombardments. The yield ratios for ^{62}Zn, ^{66}Ga, and ^{69}Ge (Fig. 3) appear to be enhanced in the ^{14}N irradiation by factors of 3–5. It is known,[40,41] however, that products of charge greater than that of the target can be formed by secondary reactions of protons, α particles, etc. For example, the ^{65}Zn observed in the present proton irradiations can be produced by a (p, n) reaction of low-energy protons (the peak cross section is 730 mb at 11 MeV).[42] We have not performed studies with different thickness targets to evaluate the ratio of primary and secondary reactions leading to such products, but data for similar thickness targets[41] indicate a major fraction of the yields of ^{62}Zn, ^{65}Zn, and ^{66}Ga (and probably ^{69}Ge) observed in the proton irradiations is of secondary origin. Note for example the very similar dependence of ^{3}H and ^{65}Zn yields on position in the target stack as shown in Table V.

The targets used for the ^{14}N irradiation were $\approx$5 times thicker than those used for the proton irradiations. Other factors being equal, we expect the yield of secondary reactions to be enhanced by less than this factor.[41] (The apparent cross section would become independent of thickness for targets appreciably thicker than the range of the secondary particles.) The experimental values of the ratios for ^{62}Zn, ^{66}Ga, and ^{69}Ge are in the range 2.8 to 5.3 which might suggest some primary effect. However, we have observed (Table I and Fig. 3) that the yield of low mass products ^{3}H and ^{7}Be per interaction is greater for ^{14}N ions than for protons. Such an enhanced flux of low mass primary products is expected to enhance the production of secondary products. We feel a major part of the apparent enhancement of yields of these products is due to secondary reactions as a consequence both of the thicker target and of the higher yields of low mass products. Certainly, the rapid decrease of the yields of these heavy products with increasing mass and charge indicates that major transfers of mass or charge from the projectile are improbable. That the yield of ^{76}Br is lower by a factor of $\approx 10^3$ than typical high yield products such as ^{58}Co implies no significant contribution of an exotic compound-nucleus-like reaction which adds nearly all the ^{14}N mass to the target and still leaves the product with such a low excitation energy that it survives without extensive particle evaporation. We cannot rule out some simpler transfer reactions, e.g., equivalent to $(2p, xn)$ or (α, xn) reactions and indeed, our observation of small shifts in Z_p for products near the target is consistent with such reactions of the ^{14}N ions, but again the effects are minor.

C. Limiting fragmentation and factorization

Data now becoming available on the reactions of very-high-energy protons and heavy ions with complex nuclei show strong similarities to patterns observed in elementary particle interactions. As a consequence, it may be useful to discuss the reactions of complex nuclei in terms of the limiting hypotheses which have been proposed to account for features of high-energy multiparticle reactions.[43]

Consider the reaction

$$a + b \rightarrow c + X, \tag{6}$$

where a is the target particle or nucleus having a four momentum p_a, b is the projectile particle or nucleus with a four momentum p_b, c is some product selected for study having four momentum components $q_{\parallel}$ and $q_{\perp}$, and X represents everything else. If we define a reduced cross section for reaction (6) as

$$F_{ab}^{c}(q_{\parallel}, q_{\perp}, s) = E\frac{\partial^2\sigma}{\partial q_{\parallel}\partial q_{\perp}}, \tag{7}$$

where E is the total energy of c and $s = (p_a + p_b)^2$, the hypothesis of limiting fragmentation asserts that $F_{ab}^{c}(q_{\parallel}, q_{\perp}, s)$ will, for fixed $q_{\parallel}$, approach a limit which is independent of s for large s, or equivalently, for very high bombarding energies. Such considerations in either the target or projectile rest frames define reactions as either target or projectile fragmentation. We expect to see energy independent spectra and cross sections in this asymptotic limit.

A second useful concept is that of *factorization* which can be developed from considerations of inclusive reactions. For high energies, this states that the reduced cross section for forming c will depend on the nature of b only via a total cross section term, i.e.,

$$F_{ab}^{c} = \sigma_{ab}\gamma_{a}^{c}(q_{\parallel}, q_{\perp}), \tag{8}$$

where σ_{ab} is the total cross section for b reacting with a and γ_a^c is a factor describing the production of c from a independently of the nature of b. For low values of $q_{\parallel}$ (correlated with p_a) Eq. (8) applies to target fragmentation. Similar results may be derived for beam fragmentation by considerations in the projectile frame. We expect to see target fragmentation spectra and cross sections independent of the beam (except for a total cross section) and projectile fragmentation spectra and cross sections independent of target.

For reactions of protons with complex nuclei, data appear to indicate the limiting fragmentation region is reached at energies between ≈6 and ≈30 GeV. For example, changes in spallation yield patterns between 30 and 300 GeV are small,[44-46] and spectra of some reaction products appear to have reached limits in the 6–10-GeV range.[46,47]

Only limited data are available for heavy ion induced reactions. Heckman's observation[4] that the relative yields and spectra of beam fragmentation products do not depend on the nature of the target led him to conclude that factorization applied for 29-GeV ^{14}N ions.

On the other hand, Katcoff and Hudis[7] have concluded that the ratio of fission cross section to total cross section is larger for 29-GeV ^{14}N ions incident on heavy elements than the corresponding ratio for 29-GeV protons. If fission is considered as a form of target fragmentation, one must conclude the limiting values have not yet been reached for 29-GeV ^{14}N ions. However, their results do show that momentum transfer in fission induced by 29-GeV ^{14}N ions is comparable to that observed for protons at the same energy.

The general similarity ot the yield patterns for 3.9-GeV ^{14}N ions and protons observed in the present work can be considered as giving support to the factorization hypothesis. That the ratios plotted in Fig. 3 are constant to $\approx \pm 25\%$ for a wide range of products from ^{64}Cu to ^{24}Na is quite striking. It should be further noted that while the slope of the proton spallation yield curve [the X_4 parameter of Eq. (5)] is probably near its limiting value, the value for ^{14}N ions may continue to decrease which would make the ratios even more constant. Either this is a remarkable accident or it is evidence for factorization. A key test would be a similar study with higher energy ^{14}N ions such as the 29-GeV ^{14}N ions that will be available at the Bevalec. Meson production in the individual interactions between projectile and target nucleons is expected to play a much more important role at 2.1 GeV/amu than it does at 278 MeV/amu. If changes in the spallation yield patterns for ^{14}N were found to be as pronounced as those observed for protons between 278 MeV and 2.1 GeV, factorization would certainly not be justified.

Results on light fragment production present some problems when discussed in terms of limiting hypotheses. There is naturally the problem of resolving beam and target fragmentation. If we focus on what is probably mostly target fragmentation, the results of Sullivan *et al.*[8] for 34-GeV ^{16}O ions (2.1 GeV/amu) on Au indicated enhanced cross sections and different spectra (lower mean charges and kinetic energies and broader spectra) than observed for 2.1- or 5.5-GeV protons.[48] While one might argue that the correct comparison would be with still higher-energy protons, such data are not yet available. However, the relative ^{3}H production cross section determined in the present work for 3.9-GeV ^{14}N ions on copper (Table I) appears to be higher than the equivalent proton values for all energies up to 25 GeV (Table VI).

The concepts of limiting fragmentation and factorization, borrowed from elementary particle physics, seem to offer interesting possibilities as an essentially macroscopic description of nuclear reactions between very-high-energy protons or heavy ions and complex nuclei (as compared to Monte Carlo calculations which examine intranuclear cascades in fine detail). At the present time, data are too sparse to draw firm conclusions as to the range of validity of these ideas. However, they are useful both as a framework for discussing existing experimental results and for indicating areas for further exploration.

ACKNOWLEDGMENTS

The authors wish to express their appreciation to K. Krien for assistance during the early phases of this experiment, to E. Rowland and M. Kinney for help in the data acquisition and analysis, and to E. Norton for the chemical yield determinations. We are particularly indebted to R. F. Peierls for stimulating discussions of limiting fragmentation and factorization and to Y. Y. Chu, G. Friedlander, J. Hudis, and S. Katcoff for their helpful comments on our manuscript. We owe a special debt to M. G. White. Without his efforts we would not have had an operational PPA at the time of our experiment.

APPENDIX

The basic data from the present experiment consisted of a large set of counting rates at the ends of the irradiations for the various radiations of the isotopes of interest. These were converted to disintegration rates by application of corrections for detector efficiency (including summing corrections) and radiation abundance, and finally relative or absolute cross sections were derived which included corrections for temporal variations of the beam. Values of half-lives, energies, and radiation abundances used for these calculations are listed in Table VII. β-ray branches were obtained from existing compilations.[16] γ-ray abundances were taken from Wakat's table[49] with a few major exceptions as indicated. In general only the stronger transitions could be used in the low intensity ^{14}N irradiation.

Abundances for the 373-, 397-, and 617-keV γ rays of ^{43}K were calculated from the data of

TABLE VII. Nuclear properties used in the analysis of the present experiments.

Isotope	Half-life	Radiation	Abundance [a]	Isotope	Half-life	Radiation	Abundance [a]
^{3}H	12.33 yr	β	1.00	^{52}Mn	5.7 day	744	0.88
^{7}Be	53 day	477	0.103			936	0.94
^{22}Na	2.62 yr	1275	1.00			1434	1.00
^{24}Na	15.0 h	1368	1.00			β	0.283
		2754	1.00	^{52}Mn^{m}	21.4 min	1434	0.98
		β	1.00	^{59}Mn	303 day	835	1.00
^{27}Mg	9.5 min	844	0.72	^{56}Mn	2.58 h	847	0.99
		1014	0.28			1811	0.30
^{28}Mg	21.0 h	401	0.36			2112	0.15
		1342	0.54	^{52}Fe	8.2 h	1434	0.98
		1779 (^{28}Al)	1.00	^{53}Fe	8.5 min	377	0.38[g]
^{29}Al	6.6 min	1273	0.94	^{59}Fe	45 day	1099	0.565
^{34}Cl^{m}	32.0 min	146	0.360[b]			1292	0.432
		2128	0.484[b]	^{55}Co	18.2 h	477	0.163
^{38}Cl	37.3 min	1643	0.35			931	0.73
		2167	0.47			1408	0.18
^{39}Cl	55.5 min	1267	0.50			β	0.789
		1517	0.42	^{56}Co	77.3 day	847	1.00
^{37}Ar	34.4 day	EC	1.00			1038	0.129
^{39}Ar	269 yr	β	1.00			1238	0.666
^{41}Ar	1.83 h	1294	0.99	^{57}Co	270 day	122	0.859
^{42}Ar	32.9 yr	β (^{42}K)	1.00			136	0.106
^{38}K	7.71 min	2167	1.00	^{58}Co	71.3 day	811	0.99
^{42}K	12.4 h	1525	0.18	^{60}Co	5.26 yr	1173	1.00
		β	1.00			1332	1.00
^{43}K	22.4 h	373	0.872[c]	^{61}Co	1.65 h	67	0.90
		397	0.114[c]			β	1.00
		617	0.805[c]	^{62}Co	13.9 min	1163	0.738[h]
		β	1.000			1173	1.00[h]
^{44}K	22 min	1157	0.582[d]	^{56}Ni	6.1 day	159	1.00
^{47}Ca	4.53 day	1297	0.76	^{57}Ni	36.0 h	128	0.15
^{43}Sc	3.92 h	373	0.22			1378	0.849
^{44}Sc^{m}	2.44 day	270	0.86	^{65}Ni	2.56 h	1482	0.25
		1157 (^{44}Sc^{g})	1.072[e]	^{60}Cu	23.4 min	467	0.057[i]
		β	0.95			826	0.217[i]
^{44}Sc^{g}	3.92 h	1157	1.00			1332	0.88[i]
^{46}Sc	83.9 day	889	1.00			1792	0.454[i]
		1120	1.00	^{61}Cu	3.41 h	67	0.057
^{47}Sc	3.43 day	159	0.73			284	0.11
		β	1.00			656	0.097
^{48}Sc	43.8 h	983	1.00			1185	0.04
		1038	1.00			β	0.632
		1312	1.00	^{64}Cu	12.75 h	β	0.585
^{48}V	16.0 day	983	1.00	^{62}Zn	9.15 h	β	1.124[e]
		1312	0.97	^{63}Zn	38.4 min	670	0.085[j]
^{48}Cr	22.96 h	113	0.98	^{65}Zn	245 day	1115	0.49
		308	0.99	^{65}Ga	15.0 min	115	0.55
^{49}Cr	41.9 min	62	0.174[f]	^{66}Ga	9.4 h	β	0.55
		91	0.539[f]	^{69}Ge	39.2 h	β	0.35
		153	0.295[f]	^{76}Br	16.0 h	β	0.50
^{51}Cr	27.8 day	320	0.098				

[a] γ-ray abundances are taken from Wakat, Ref. 49, except where indicated; β abundances from Ref. 16.
[b] From Ref. 54.
[c] From Ref. 50.
[d] From Ref. 55.
[e] Includes correction for genetic relationship
[f] From Ref. 51.
[g] From Ref. 53.
[h] From Ref. 56.
[i] From Ref. 58.
[j] From Ref. 57.

TABLE VIII. Individual cross sections for forming $^{44}Sc^{m}$ by irradiations of ^{63,65}Cu with 3.9-GeV ^{14}N ions and protons.

Radiation	Laboratory	^{14}N cross section (relative units)	Proton cross section (mb)
270 keV	BNL	4.30 ± 0.10	5.17 ± 0.10
270 keV	PU	4.03 ± 0.12	5.46 ± 0.16
1157 keV	BNL	4.28 ± 0.12	5.02 ± 0.11
1157 keV	PU	4.21 ± 0.22	5.27 ± 0.16
β	BNL	4.30 ± 0.20	6.34 ± 0.40
Mean		4.22 ± 0.06	5.22 ± 0.06
FIT [a]		0.78	1.86

[a] See text for definition.

TABLE IX. Individual cross sections for forming ^{48}Cr by irradiations of ^{63,65}Cu with 3.9-GeV ^{14}N ions and protons.

Radiation	Laboratory	^{14}N cross section (relative units)	Proton cross section (mb)
113 keV	BNL	0.29 ± 0.02	0.30 ± 0.01
113 keV	PU	0.18 ± 0.02 [a]	0.31 ± 0.01
308 keV	BNL	0.34 ± 0.05	0.33 ± 0.01
308 keV	PU	0.38 ± 0.09	Not reported
Mean		0.30 ± 0.02	0.31 ± 0.005
FIT [b]		0.90	1.71

[a] Not included in mean.
[b] See text for defnition.

Waters[50] with the assumption of 1.3% decay to the ground state of ^{43}Ca.

Cross sections for ^{49}Cr calculated using Wakat's abundances for the 61-, 92-, and 153-keV γ rays showed a spread of a factor of 2, and gave a mean value which appeared anomalous when compared to neighboring species. When abundances from the recent study by Okon *et al.*[51] were used, cross sections calculated from the three transitions were the same within 5%, and the mean was consistent with systematics. This casts suspicion on the work of Adams and Dams[52] which served as Wakat's original reference. Since Wakat's abundance for the 377-keV γ ray of ^{53}Fe also was based on these authors,[52] we prefer to use the abundance given by Auble and Rao.[53]

Several additional discrepancies were observed in which Wakat apparently quoted relative intensities, or neglected feeding of a level by other transitions. In these cases, $^{34}Cl^{m}$, ^{44}K, ^{62}Co, ^{63}Zn, and ^{60}Cu, values from the original sources[54-58] were used.

For each bombarding particle and irradiation, a mean cross section was calculated from the individual values, weighting them by the reciprocals of the squares of their standard deviations. A quantitative measure of the internal agreement of such a data set is given by FIT which is defined as

$$\mathrm{FIT} = \left[\frac{1}{n-1} \left(\sum_{i=1}^{n} \frac{\Delta_i}{\sigma_i} \right)^2 \right]^{1/2},$$

where σ_i and Δ_i are the standard deviation and deviation from the mean of the ith datum, respectively, and n is the number of values included in the average. If the standard deviations are good measures of the precision of the individual values, FIT is expected to be unity. In those cases of poor fits, individual values were carefully examined for sources of discrepancies. Where effects such as abnormal decay curves or interfering γ rays were found, an occasional value was rejected and a revised mean and FIT calculated. In some cases, poor fits seemed to be due probably to uncertainties in γ-ray abundances.

It is instructive to examine a few specific cases which illustrate the above procedures. Results for $^{44}Sc^{m}$ are presented in Table VIII. This species (half-life 2.44 day) could be assayed readily via its 270-keV γ ray or by the 1157-keV γ ray in the 3.92-h daughter, as well as by β counting where it is a major component of the Sc decay curve. For the ^{14}N irradiation, a FIT of 0.78 indicates good agreement between observed deviations and the estimated errors. In the case of the proton irradiation, FIT = 1.86, and the agreement is somewhat poorer than indicated by the individual error estimates. It can be seen that this situation would have been even worse had the individual errors not been enlarged by the 2% in the case of the γ counts and 4% for the β counts. However, we are dealing with measurements of rather high precision, the standard error of the mean being only a little over 1%. We have observed this effect in many of the more precise assays in this work. When the statistical errors become small, the internal agreement of points as measured by FIT becomes poorer. We have adopted the convention of multiplying the standard error of the mean by FIT for those cases where FIT is greater than unity, e.g., the cross section for producing $^{44}Sc^{m}$ by protons is reported as 5.22 ± 0.11 mb in Table I. In general, a precision of better than 2% cannot be attained even by combining measurements on different γ rays from different laboratories.

As might have been expected, other factors being equal, assay of species formed in low yield proved to be more difficult than assay of those formed in high yields. This was particularly true where the γ rays from the isotope came only at low energies

on top of the Compton distribution of the intense annihilation radiation. Data for a representative example, ^{48}Cr, are presented in Table IX. Both the 113- and 308-keV γ-ray lines, though abundant in the decay scheme, are in a spectral region of high background. Three measurements with modest agreement (FIT = 1.71) give a mean cross section of 0.31 ± 0.01 mb for the proton irradiation. However, for ^{14}N, the results from PU for the 113-keV line appear to be abnormally low. If all four values had been included, the average would have been 0.25 ± 0.01, with a poor FIT of 2.58. The decay of the 113-keV line as resolved from the PU spectra showed a large amount of a short-lived component which was initially assigned to ^{65}Ga, and then a poorly defined tail of half-life $\approx$14 h compared to the expected value 23 h. The apparent ^{65}Ga cross section (Table I) derived from this analysis was anomalously high and we believe there were serious difficulties in resolving this γ-ray line.

The last case we will discuss in detail is ^{61}Cu. Although this species is formed in high yield, the low abundance of the γ rays in its decay (Table VII) and its relatively short (3.41 h) half-life apparently lead to difficulties in accurate assay. Seven measurements of the cross section for forming ^{61}Cu by proton irradiation are given in Table X. The value obtained from measurements of the 67-keV γ ray is seen to be substantially lower than the other six. A trouble of this sort was not unexpected as the decay of this γ line is dominated by ^{61}Co (half-life 1.7 h). Only 5% of the initial counting rate of the 67-keV peak is due to ^{61}Cu. Furthermore, the abundance of this γ ray in the decay of ^{61}Cu is known to only $\pm$25%. As a consequence we have not included the 67-keV result in the average. Even with this value removed there is still a spread of some 25% in the remaining values leading to a FIT of 3.17 when they are averaged. It is interesting to note that if the abundance (0.13) adopted by Vervier[59] had been used rather than the 0.11 of Wakat, the cross sections reported by BNL and PU based on the 284-keV γ ray would have been reduced to 10.7 and 10.2 mb, respectively. A major part of the observed spread may be due to uncertainties in the γ-ray abundances. In the case of the ^{14}N irradiation, the relatively poor agreement (FIT = 2.57) of the measurements is more probably due to difficulties in resolving the γ lines from the spectra at the lower counting rates. We have included the result from the β measurement only to illustrate a point. ^{61}Cu is isotopic with the target and even if a thick counting sample is accepted, only a small fraction (3%) of the total ^{61}Cu activity could be mounted for assay. Decay prior to the start of the assay, the low counting rate, and large uncertainties in the counting efficiency of the thick sample all contribute to the large uncertainty of the β value.

TABLE X. Individual cross sections for forming ^{61}Cu in irradiations of ^{63,65}Cu with 3.9-GeV ^{14}N ions and protons.

Radiation	Laboratory	^{14}N cross section (relative units)	Proton cross section (mb)
67 keV	BNL	Not reported	6.9 ± 0.4 [a]
284 keV	BNL	12.6 ± 0.4	12.7 ± 0.3
284 keV	PU	Not reported	12.1 ± 0.4
656 keV	BNL	15.2 ± 0.6	11.3 ± 0.3
656 keV	PU	15.1 ± 0.8	11.4 ± 0.4
1185 keV	BNL	11.6 ± 1.3	9.9 ± 0.3
β	BNL	6.8 ± 1.5 [a]	10.2 ± 0.5
Mean		13.7 ± 0.3	11.5 ± 0.13
FIT [b]		2.57	3.17

[a] Not included in mean.
[b] See text for definition.

*Research performed under the auspices of the U. S. Atomic Energy Commission.
†Present address: Chemistry Department, Yale University, New Haven, Connecticut 06520.

[1]M. G. White, M. Isaila, K. Prelec, and H. L. Allen, Science, 174, 1121 (1971).
[2]H. A. Grunder, W. D. Hartsough, and E. J. Lofgren, Science 174, 1128 (1971).
[3]H. H. Heckman, D. E. Greiner, P. J. Lindstrom, and F. S. Bieser, Science 174, 1130 (1971).
[4]H. H. Heckman, D. E. Greiner, P. J. Lindstrom, and F. S. Bieser, Phys. Rev. Lett. 28, 926 (1972).
[5]C. A. Tobias, J. T. Lyman, A. Chatterjee, J. Howard, M. D. Maccabee, M. R. Raju, A. R. Smith, J. M. Sperinde, and G. P. Welch, Science 174, 1131 (1971).
[6]C. A. Tobias, A. Chatterjee, and A. R. Smith, Phys. Lett. 37A, 119 (1971).
[7]S. Katcoff and J. Hudis, Phys. Rev. Lett. 28, 1066 (1972); private communication.
[8]J. D. Sullivan, P. B. Price, H. J. Crawford, and M. Whitehead, Phys. Rev. Lett. 30, 136 (1973).
[9]A notable exception is the measurement of the ^{12}C(^{14}N, x)-^{11}C cross section at 3.8 GeV by L. Skoski, M. Merker, and B. S. P. Shen, Phys. Rev. Lett. 30, 51 (1973).
[10]Spectrographic analysis indicated that the most significant impurity was $\approx$ 0.01% Ag.
[11]W. Schimmerling, K. G. Vosburgh, and P. W. Todd, Science 174, 1123 (1971).
[12]J. F. Janni, Air Force Weapons Laboratory Report No. AFWL-TR 65-150 (Research and Technology Division,

Air Force Systems Command, Kirtland Air Force Base, New Mexico, 1966).
[13]J. B. Cumming, National Academy of Sciences - National Research Council, Nuclear Science Series Report No. NAS-NS-3107, 1962 (unpublished).
[14]R. Gunnink, H. B. Levy, and J. B. Niday, University of California Radiation Laboratory Report No. UCID-15140 (unpublished); modified by B. R. Erdal (unpublished).
[15]E. Storm and H. I. Israel, Nucl. Data A7, 565 (1970).
[16]C. M. Lederer, J. M. Hollander, and I. Perlman, *Table of Isotopes* (Wiley, New York, 1967), 6th ed.; Nucl. Data B1 to B3 (1966–1970).
[17]J. B. Cumming, Annu. Rev. Nucl. Sci. 13, 261 (1963).
[18]J. Hudis, I. Dostrovsky, G. Friedlander, J. R. Grover, N. T. Porile, L. P. Remsberg, R. W. Stoenner, and S. Tanaka, Phys. Rev. 129, 434 (1963).
[19]J. M. Miller and J. Hudis, Annu. Rev. Nucl. Sci. 9, 159 (1959).
[20]J. Hudis, in *Nuclear Chemistry*, edited by L. Yaffe (Academic, New York, 1968), pp. 169-272.
[21]P. J. Karol, Phys, Rev. C 10, 150 (1974).
[22]C. J. Orth, H. A. O'Brien, M. E. Schillaci, B. J. Dropesky, J. E. Cline, E. B. Nieschmidt, and R. L. Brodzinski, as quoted in Ref. 21.
[23]G. Rudstam, Z. Naturforsch. 21a, 1027 (1966).
[24]Y. Y. Chu, E. M. Franz, G. Friedlander, and P. J. Karol, Phys. Rev. C 4, 2202 (1971).
[25]G. T. Garvey, W. J. Gerace, R. L. Jaffe, I. Talmi, and I. Kelson, Rev. Mod. Phys. 41, S1 (1969).
[26]Formulas used in the present work are expressed in terms of $(A-50)$ rather than A as this kept the range of terms in more reasonable bounds when higher powers were included.
[27]D. Barr, University of California Radiation Laboratory Report No. UCRL-3793, 1957 (unpublished). Original cross sections have been multiplied by the factor 8.7/10.5 to correct for a revised monitor cross section value, Ref. 17.
[28]L. Husain and S. Katcoff, Phys. Rev. C 7, 2452 (1973).
[29]G. Friedlander, J. M. Miller, R. Wolfgang, J. Hudis, and E. Baker, Phys. Rev. 94, 727 (1954); J. Hudis, T. Kirsten, R. W. Stoenner, and O. A. Schaeffer, Phys. Rev. C 1, 2019 (1970).
[30]N. Metropolis, R. Bivins, M. Storm, J. M. Miller, G. Friedlander, and A. Turkevich, Phys. Rev. 110, 204 (1958).
[31]V. Schwarz and H. Oeschger, Z. Naturforsch. 22a, 972 (1967).
[32]V. P. Crespo, J. M. Alexander, and E. K. Hyde, Phys. Rev. 131, 1765 (1963).
[33]N. T. Porile and S. Tanaka, Phys. Rev. 135, B122 (1964); 137, B58 (1965).
[34]Range-energy curves for ^{3}H and ^{7}Be in copper were derived from the data of Janni, Ref. 12, by multiplying proton ranges at the same velocity by A/Z^2.
[35]L. A. Currie, W. F. Libby, and R. L. Wolfgang, Phys. Rev. 101, 1557 (1956).
[36]K. Goebel, H. Schultes, and J. Zähringer, CERN Report No. CERN 64-12, 1964 (unpublished).
[37]V. V. Kuznetsov and V. N. Mekhedov, J. Exp. Theor. Phys. (USSR) 35, 587 (1959) [transl.: Sov. Phys. JETP 35, 406 (1959)].
[38]T. A. Kirsten and O. A. Schaeffer, in *Interactions of Elementary Particle Research in Science and Technology*, edited by L. C. L. Yuan (Academic, New York, 1971).
[39]J. R. Grover and A. A. Caretto, Jr., Annu. Rev. Nucl. Sci. 14, 51 (1964).
[40]A. Turkevich and N. Sugarman, Phys. Rev. 94, 728 (1954).
[41]G. Rudstam, Nucl. Phys. 56, 593 (1964).
[42]R. Collé, R. Kishore, and J. B. Cumming, Phys. Rev. C 9, 1819 (1974).
[43]See the review by W. R. Frazer, L. Ingber, C. H. Mehta, C. H. Poon, D. Silverman, K. Stowe, P. D. Ting, and H. J. Yesian, Rev. Mod. Phys. 44, 284 (1972).
[44]S. Katcoff, S. B. Kaufman, E. P. Steinberg, M. W. Weisfield, and D. B. Wilkins, Phys. Rev. Lett. 30, 1221 (1973).
[45]G. English, Y. W. Yu, and N. T. Porile, Phys. Rev. Lett. 31, 244 (1973).
[46]S. K. Chang and N. Sugarman, Phys. Rev. C 3, 1138 (1974).
[47]K. Beg and N. T. Porile, Phys. Rev. C 3, 1631 (1971).
[48]A. M. Poskanzer, G. W. Butler, and E. K. Hyde, Phys. Rev. C 3, 882 (1971).
[49]M. A. Wakat, Nucl. Data A8, 445 (1971).
[50]S. L. Waters, Radiochim Acta 17, 63 (1972).
[51]O. B. Okon, H. Bakhru, M. K. Dewanjee, and I. L. Preiss, Phys. Rev. C 7, 239 (1973).
[52]F. Adams and R. Dams, J. Radioanal. Chem. 3, 271 (1969).
[53]R. L. Auble and M. N. Rao, Nucl. Data B3 (No. 5, 6), 127 (1970).
[54]T. E. Ward and P. K. Kuroda, J. Inorg. Nucl. Chem. 33, 609 (1971).
[55]H. Ing, J. D. King, R. L. Schulte, and H. W. Taylor, Nucl. Phys. A203, 164 (1973).
[56]J. N. Mo, S. Ray, and S. K. Mark, Nucl. Phys. A125, 440 (1969).
[57]J. R. Van Hise and D. C. Camp, Phys. Rev. Lett. 23, 1248 (1969).
[58]I. Borchert, Z. Phys. 223, 473 (1969).
[59]J. Vervier, Nucl. Data B2 (No. 5), 81 (1968).